EuroIntervention 2018;13:2036-2046 published online July 2017

The drug-eluting resorbable magnesium vascular scaffold in complex coronary bifurcations: insights from an in vivo multimodality imaging study

Johan Bennett[1,2]*, MB, BCh, MD; Maarten Vanhaverbeke[1,2], MD; Nina Vanden Driessche[2], BSc; Nick Hiltrop[1], MD; Tom Adriaenssens[1,2], MD, PhD; Walter Desmet[1,2], MD, PhD; Peter Sinnaeve[1,2], MD, PhD; Christophe Dubois[1,2], MD, PhD

1. Department of Cardiovascular Medicine, University Hospitals Leuven, Leuven, Belgium; 2. Department of Cardiovascular Sciences, Katholieke Universiteit Leuven, Leuven, Belgium

This paper also includes supplementary data published online at: http://www.pcronline.com/eurointervention/132nd_issue/333

KEYWORDS

- bifurcation
- bioresorbable scaffolds
- optical coherence tomography

Abstract

Aims: This acute *in vivo* study sought to provide insights regarding the feasibility of performing complex bifurcation stenting with Magmaris magnesium alloy bioresorbable scaffolds (Biotronik, Bulach, Switzerland).

Methods and results: Twenty-five New Zealand White rabbits underwent stenting of non-diseased aorto-iliac bifurcations with the Magmaris using provisional (PS; n=5), culotte (n=6), modified T (n=6), or T and protrusion (TAP, n=8) stenting techniques. Angiography, optical coherence tomography and micro-computed tomography were performed. Angiographic results were good without evidence of side branch (SB) compromise. In 9/25 procedures, strut fractures were identified with minimal luminal compromise in two cases. PS opened the SB optimally without evidence of scaffold compromise. Culotte resulted in complete bifurcation coverage and good scaffold expansion; single strut fractures were present in three out of six and double fractures in one out of six procedures. Modified T and TAP resulted in complete bifurcation coverage, minimal neocarina double-strut layers and good expansion. In two out of six modified T procedures, strut fractures were present with SB scaffold deformity present in an additional two out of six procedures. In three out of eight TAP procedures, strut fractures were present without compromising overall scaffold integrity.

Conclusions: Bifurcation stenting using Magmaris appears feasible. PS with additional TAP whenever needed seems a reasonable approach. Whenever a two-stent technique is planned, TAP appears most favourable whilst modified T and culotte stenting should probably be avoided.

**Corresponding author: Department of Cardiovascular Medicine, University Hospitals Leuven, Herestraat 49, B-3000 Leuven, Belgium. E-mail: johan.bennett@uzleuven.be*

SUBMITTED ON 27/03/2017 - REVISION RECEIVED ON 1st 12/06/2017 / 2nd 04/07/2017 - ACCEPTED ON 21/07/2017

DOI: 10.4244/EIJ-D-17-00248

Abbreviations

BRS	bioresorbable scaffold(s)
BVS	bioresorbable vascular scaffold(s)
DES	drug-eluting stent(s)
ISA	incomplete strut apposition
micro-CT	micro-computed tomography
mini-KBPD	mini-kissing balloon post-dilatation
MV	main vessel
NC	non-compliant
OCT	optical coherence tomography
POT	proximal optimisation technique
PS	provisional stenting
RMS	resorbable magnesium scaffold
SB	side branch
TAP	T and protrusion

Introduction

Up to 15% of all percutaneous coronary interventions involve the treatment of coronary bifurcations[1]. Treatment of bifurcation lesions with drug-eluting stents (DES), especially when a double-stent technique is used, is associated with a higher risk for stent restenosis and thrombosis[2]. Bioresorbable scaffolds (BRS) may offer potential advantages compared with metallic DES, aiming at restoring vessel patency without implanting a permanent device. Furthermore, after scaffold bioresorption, potentially no residual triggers for late stent thrombosis would be present.

There are currently two polymer-based scaffolds on the market: the Absorb™ bioresorbable vascular scaffold (BVS) (Abbott Vascular, Santa Clara, CA, USA) and the DESolve® (Elixir Medical Corporation, Sunnyvale, CA, USA). More recently, a third bioresorbable scaffold, the magnesium-based Magmaris™ (Biotronik AG, Bülach, Switzerland), obtained CE marking.

The feasibility of using Absorb BVS in complex bifurcation techniques has been investigated in *ex vivo* investigations[3] and, more recently, by our group, in an *in vivo* rabbit bifurcation model with correlation of angiography, optical coherence tomography (OCT) and micro-computed tomography (micro-CT)[4].

At present, there are no clinical, *ex vivo* or *in vivo* data available on the feasibility and safety of using the DESolve BRS or the Magmaris resorbable magnesium scaffold (RMS) in complex bifurcation stenting. The Magmaris presents a promising BRS for use in complex interventions as the magnesium material is more deliverable, as compared to the polymeric Absorb[5], more robust, and can potentially provide higher radial strength for dilating atherosclerotic lesions, and hence greater acute lumen gain[6]. In addition, it would theoretically allow more optimal post-dilatation, post-dilatation to larger diameters and more aggressive kissing balloon dilatations to ensure optimal expansion, without increased risk of strut fracture or compromise of scaffold integrity. Nevertheless, the integrity of the magnesium scaffold may be compromised, resulting in multiple strut fractures, by common techniques required during two-stent bifurcation techniques such as recrossing, proximal optimisation and kissing balloon post-dilatation (KBPD).

We investigated the feasibility of using Magmaris RMS in commonly used simple (provisional) and complex (T and protrusion, modified T and culotte) bifurcation procedures.

The results of this *in vivo* study, using multimodality imaging to assess acute scaffold integrity, will provide insights to aid the application of this novel scaffold to diseased human coronary bifurcations.

Methods

The study was approved by the Ethics Committee for Animal Experimentation (KU Leuven, Belgium). The experiments were performed in an *in vivo* rabbit non-diseased aorto-iliac bifurcation model, as previously described[4]. Under general anaesthesia, twenty-seven New Zealand White (NZW) rabbits (weight 3.5-4.5 kg) underwent bifurcation interventions of the aorto-iliac bifurcation. The vessel diameters of distal aorta and iliac arteries in the NZW rabbit are suitable for implantation of 3.0 mm scaffolds, allowing proximal optimisation in the aorta up to 3.5 mm. The bifurcation has an angle of approximately 70%, as measured from the axis of the main vessel (MV; determined as aorta to right iliac artery) to the axis of the origin of the side branch (SB; determined as the left iliac artery). Arterial access was achieved by denuding the carotid artery and introducing a 45 cm 6 Fr Check-Flo® Introducer (Cook Medical, Bloomington, IN, USA) to the distal descending aorta. Intra-arterial heparin (5,000 IU) was administered.

The Magmaris, formerly known as DREAMS 2G, is made of a proprietary magnesium alloy coated with a poly-L-lactic acid (PLLA) biodegradable polymer eluting sirolimus (1.4 µg/mm^2 of scaffold surface)[6]. The scaffold design **(Figure 1)** consists of six in-phase sinusoidal hoops/rings linked by two straight mid-strut connectors (six-crown two-link open cell design), with both strut thickness and width of 150 µm. There are tantalum radiopaque markers at both ends. The cell perimeter (**Figure 1**, broken red line) is 19.3 mm for the 3.0 mm scaffold and 20.6 mm for the 3.5 mm scaffold, as compared to 9.4 mm and 11.4 mm for the

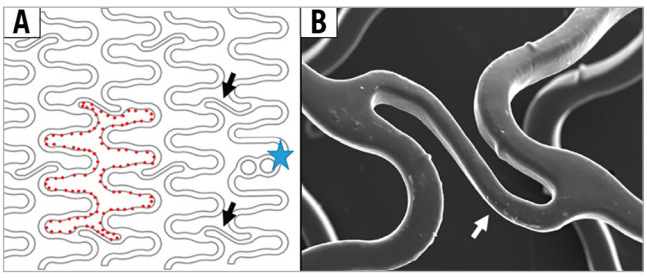

Figure 1. *Magmaris scaffold design. A) In-phase sinusoidal rings/hoops are linked by two straight connectors (black arrows), which join the hoops halfway between the peaks and valleys of the hoops. Tantalum markers are present (blue star). The broken red line delineates scaffold cell. B) High-magnification micro-CT image of mid-strut connector (white arrow), with smooth and rounded surface of scaffold struts.*

similarly sized Absorb BVS[3]. The calculated maximum circular diameter of a cell is 6.1 mm and 6.6 mm for the 3.0 mm and 3.5 mm scaffold, respectively, as compared to 3.0 mm and 3.6 mm for the similarly sized Absorb BVS. Theoretically, the more rounded and smooth Magmaris struts facilitate easier recrossing with guidewires **(Figure 1B)**. Approximately 95% of the magnesium is expected to be absorbed within 12 months.

Balance middle weight guidewires (BMW; Abbott Vascular) were used for all procedures. Semi-compliant Pantera and non-compliant (NC) Pantera balloon catheters (Biotronik AG) were used for recrossing and post-dilatation, respectively. After set-up angiography, the bifurcation procedure commenced. Following completion of the procedure and OCT examinations, the animals were sacrificed and the aorto-iliac bifurcations were extracted and stored in 50% glycerol.

BIFURCATION TECHNIQUES (Figure 2)

We performed provisional stenting (PS; n=5), culotte stenting (n=6), modified T stenting (mod-T; n=6), and T and protrusion stenting (TAP; n=8) using 3.0×25 mm Magmaris scaffolds. Proximal optimisation technique (POT) with 3.5 mm NC balloons and final kissing balloon post-dilatation (KBPD) strategies with 3.0 mm NC balloons were always performed. For all four bifurcation techniques, two predefined post-dilatation strategies were assessed, i.e., strategy 1: POT with 3.5 mm NC balloon to 16 atm and sequential post-dilatation to 14 atm followed by KBPD to 8/8 atm ("traditional" strategy); strategy 2: POT with 3.5 mm NC balloon to 16 atm and sequential post-dilatation to 14 atm, followed by mini-kissing balloon post-dilatation (mini-KBPD) at low atm (5/5 atm) ("mini" strategy)[3]. The bifurcation techniques are described in **Figure 2**.

ASSESSMENT OF THE BIFURCATION TECHNIQUES

All procedures were assessed by angiography, optical coherence tomography (OCT) (St. Jude Medical, St. Paul, MN, USA) and micro-CT (SkyScan 1076; Bruker microCT, Kontich, Belgium), as previously described[4].

STATISTICAL ANALYSIS

The data are presented as mean±SD. Differences in scaffold areas and scaffold diameters between groups were compared with the non-parametric Kruskal-Wallis test. Pairwise follow-up analysis was performed using Dunn's multiple comparison test. Statistical analyses were performed using GraphPad Prism statistical

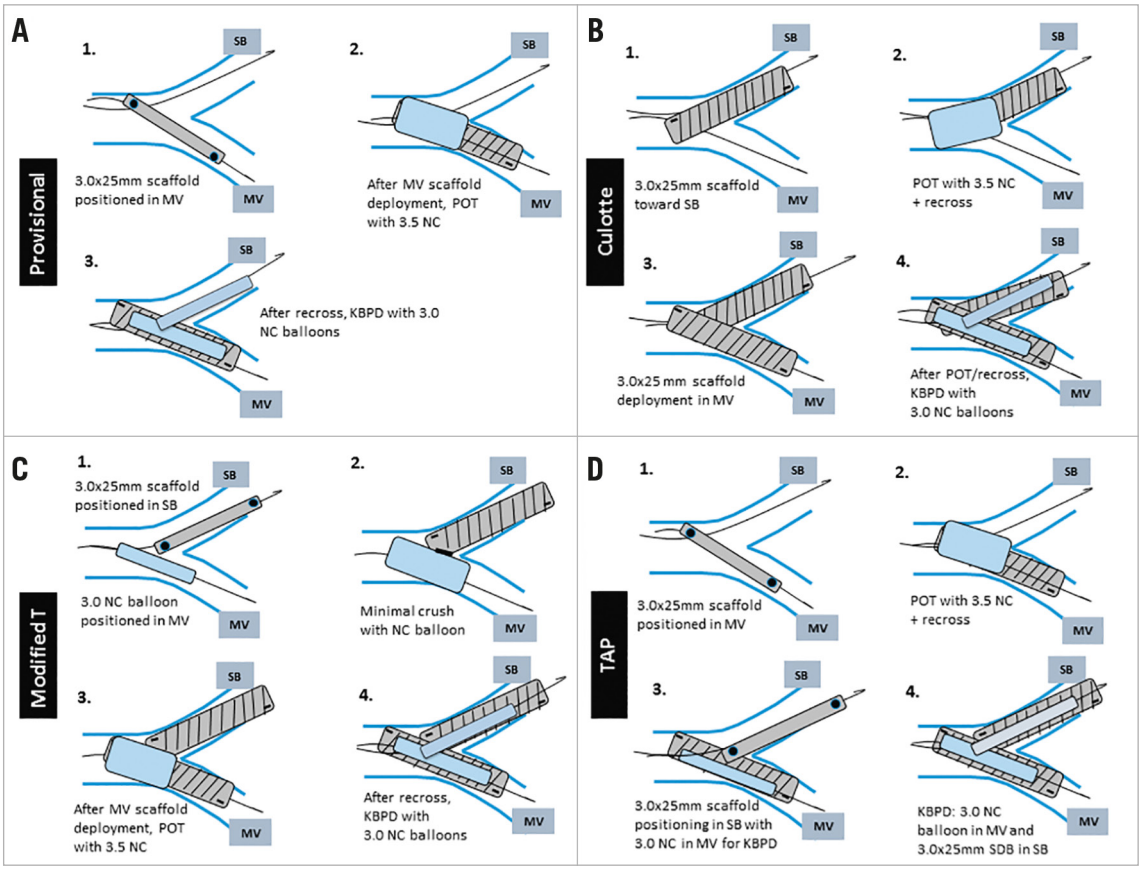

Figure 2. *Overview of main steps in bifurcation techniques. A) Provisional stenting. B) Culotte stenting. C) Modified T-stenting. D) TAP stenting. atm: atmospheres; mini-KBPD: mini-kissing balloon post-dilatation; MV: main vessel; NC: non-compliant; POT: proximal optimisation technique; SB: side branch; SDB: scaffold delivery balloon; TAP: T and protrusion*

software, version 5.01 (GraphPad Software Inc, La Jolla, CA, USA). All results were from two-sided tests and a p-value of <0.05 was considered significant.

Results

In total, 27 NZW rabbits were anaesthetised. Two experiments were terminated before stenting due to technical issues. A total of 45 Magmaris RMS were successfully delivered and implanted in 25 rabbits (provisional n=5, culotte n=6, mod-T n=6, TAP n=8) without complication, and with procedural success of 100%. In all procedures (n=25), the angiographic results were good with no dissection or SB compromise. Recrossing through the struts with guidewires was smooth. Subsequent crossing with balloons and implantation of second scaffolds (TAP+culotte procedures) were smooth, provided adequate strut dilatation was performed. Mean fluoroscopy times were: 4.8±1.0 min (PS), 9.1±1.3 min (culotte), 8.4±2.5 min (mod-T), and 5.6±1.1 min (TAP).

OPTICAL COHERENCE TOMOGRAPHY (Table 1)

There were no significant differences in luminal and abluminal minimal scaffold areas and luminal minimal scaffold diameters among the four techniques in proximal and distal MV, except for significantly larger abluminal minimal scaffold areas in the proximal MV with culotte stenting (10.8±0.5 mm^2 vs. 9.7±0.5 mm^2 with PS [p=0.018], 9.9±0.6 mm^2 with mod-T, and 10.0±0.4 mm^2 with TAP). Furthermore, despite a double strut layer in the proximal MV, the luminal scaffold area following culotte stenting (7.6±0.4 mm^2) was similar to provisional (7.6±0.6 mm^2), mod-T (7.7±0.7 mm^2), and TAP stenting (7.7±0.4 mm^2).

There were significant differences in luminal minimal scaffold area (6.4±0.5 mm^2 vs. 5.6±0.3 mm^2 vs. 5.5±0.2 mm^2, p=0.006) and luminal minimal scaffold diameter (2.8±0.1 mm vs. 2.6±0.1 mm vs. 2.6±0.0 mm, p=0.006) at the ostial SB between the TAP and the culotte and mod-T procedures, respectively, with larger luminal areas and diameters following TAP stenting. Numerically, the

Table 1. OCT findings.

		Provisional (N=5)	Culotte (N=6)	mod-T (N=6)	TAP (N=8)	*p*-value
Proximal MV	Luminal minimal scaffold area (mm^2)	7.6±0.6	7.6±0.4	7.7±0.7	7.7±0.4	ns
	Luminal minimal mean scaffold diameter (mm)	3.1±0.1	3.1±0.1	3.1±0.1	3.1±0.1	ns
	Abluminal minimal scaffold area (mm^2)	9.7±0.5	10.8±0.5	9.9±0.6	10.0±0.4	0.018
	Abluminal minimal mean scaffold diameter (mm)	3.5±0.1	3.7±0.1	3.5±0.1	3.6±0.1	ns
Distal MV (ostium)	Luminal scaffold area (mm^2)	5.7±0.5	5.8±0.2	5.7±0.2	5.8±0.2	ns
	Luminal mean scaffold diameter (mm)	2.7±0.1	2.7±0.1	2.7±0.1	2.7±0.1	ns
	Abluminal scaffold area (mm^2)	7.7±0.4	7.9±0.3	7.6±0.5	7.8±0.3	ns
	Abluminal mean scaffold diameter (mm)	3.1±0.1	3.2±0.1	3.1±0.1	3.1±0.1	ns
SB (ostium)	Luminal scaffold area (mm^2)		5.6±0.3	5.5±0.2	6.4±0.5	0.006
	Luminal mean scaffold diameter (mm)		2.6±0.1	2.6±0.0	2.8±0.1	0.006
	Abluminal scaffold area (mm^2)		7.5±0.4	7.4±0.2	8.2±0.6	ns
	Abluminal mean scaffold diameter (mm)		3.1±0.1	3.1±0.0	3.2±0.1	ns
Bifurcation core MV smallest	Luminal scaffold area (mm^2)	5.8±0.6	5.7±0.2	5.4±0.6	5.4±0.8	ns
	Luminal mean scaffold diameter (mm)	2.7±0.1	2.7±0.0	2.6±0.2	2.6±0.2	ns
	Abluminal scaffold area (mm^2)	7.7±0.4	7.7±0.3	7.4±0.8	7.6±0.3	ns
	Abluminal mean scaffold diameter (mm)	3.1±0.1	3.1±0.1	3.1±0.2	3.1±0.1	ns
Bifurcation core SB smallest	Luminal scaffold area (mm^2)		5.7±0.3	4.7±1.6	5.8±0.7	ns
	Luminal mean scaffold diameter (mm)		2.7±0.1	2.5±0.6	2.7±0.2	ns
	Abluminal scaffold area (mm^2)		7.3±0.3	7.3±0.4	7.8±0.7	ns
	Abluminal mean scaffold diameter (mm)		3.1±0.1	3.0±0.1	3.1±0.2	ns
Incompletely apposed struts	Proximal MV scaffold	1/5	4/6	5/6	4/8	
	Distal MV scaffold	2/5	3/6	3/6	4/8	
	SB scaffold		2/6	4/6	0/8	
	Bifurcation segment	5/5	6/6	6/6	8/8	
Visible strut fracture: OCT		0/5	0/6	0/6	0/8	
Strut fracture present: micro-CT		0/5	4/6	2/6	3/8	
Scaffold deformity		0/5	0/6	3/6	0/8	

micro-CT: micro-computed tomography; MV: main vessel; OCT: optical coherence tomography; SB: side branch; TAP: T and protrusion

abluminal scaffold areas and diameters were also larger following TAP stenting though this was not statistically significant.

Finally, in the bifurcation core, there were no significant differences among the four techniques with overall evidence of good scaffold expansion.

PROVISIONAL STENTING WITH KBPD (N=5) (Figure 3)

PS with KBPD opened the SB ostium optimally without deforming the MV scaffold. There was good scaffolding of the SB ostium with no detachment of the MV scaffold opposite the SB. Following all procedures, there were several incompletely apposed struts present at the bifurcation core. No strut fractures were identified.

CULOTTE STENTING WITH KBPD (N=6) (Figure 4)

In all cases, there was complete coverage of the SB ostium and carina. Inherent to the technique, culotte stenting resulted in a double layer of struts in the proximal MV. Following all procedures, there were several incompletely apposed struts present at the bifurcation core, and in four out of six cases there were several incompletely apposed struts present in the proximal MV. No definite strut fractures were identified.

MODIFIED T-STENTING WITH KBPD (N=6) (Figure 5)

In all cases, there was complete coverage of the SB ostium and carina. Modified T-stenting resulted in a layer of single struts at the carina and a short segment of double-layered struts at the proximal SB ostium. In all procedures, there were several inappropriately apposed struts at the level of the bifurcation. In two out of six procedures, there was evidence of scaffold deformity (presence of mesh of deformed elongated struts) affecting only the SB scaffold and located in the proximal MV just proximal to where the scaffold protruded from the SB **(Figure 6)**. In one further procedure, there was mild distortion of the SB scaffold due to incorrect rewiring of the SB following deployment of the MV scaffold. No definite strut fractures were identified.

T AND PROTRUSION (TAP) STENTING WITH KBPD (N=8) (Figure 7)

In seven out of eight cases, there was complete coverage of the SB ostium and carina, whilst in one case the SB scaffold was deployed too distal in the SB. TAP stenting resulted in a layer of double struts at the neocarina and a short segment of double-layered struts at the proximal SB ostium. In all procedures there were several inappropriately apposed struts at the level of the bifurcation. No definite strut fractures were identified.

THREE-DIMENSIONAL micro-CT (Table 2)

In seven out of the 25 stenting procedures, single strut fractures were identified, whilst following two procedures multiple strut fractures were identified. The majority of these fractures were only discovered following very detailed analysis of the micro-CT images and 3D reconstruction **(Figure 8)**.

Strut fractures were identified in the proximal MV following two procedures but were probably not the result of POT (in a TAP case the second scaffold was placed too proximal followed by traditional KBPD, and in a mod-T case there was definite guide catheter-induced damage). No strut fractures were identified in the distal MV or SB.

The majority of strut fractures occurred at the level of the bifurcation affecting either the MV scaffold (n=3), SB scaffold (n=3),

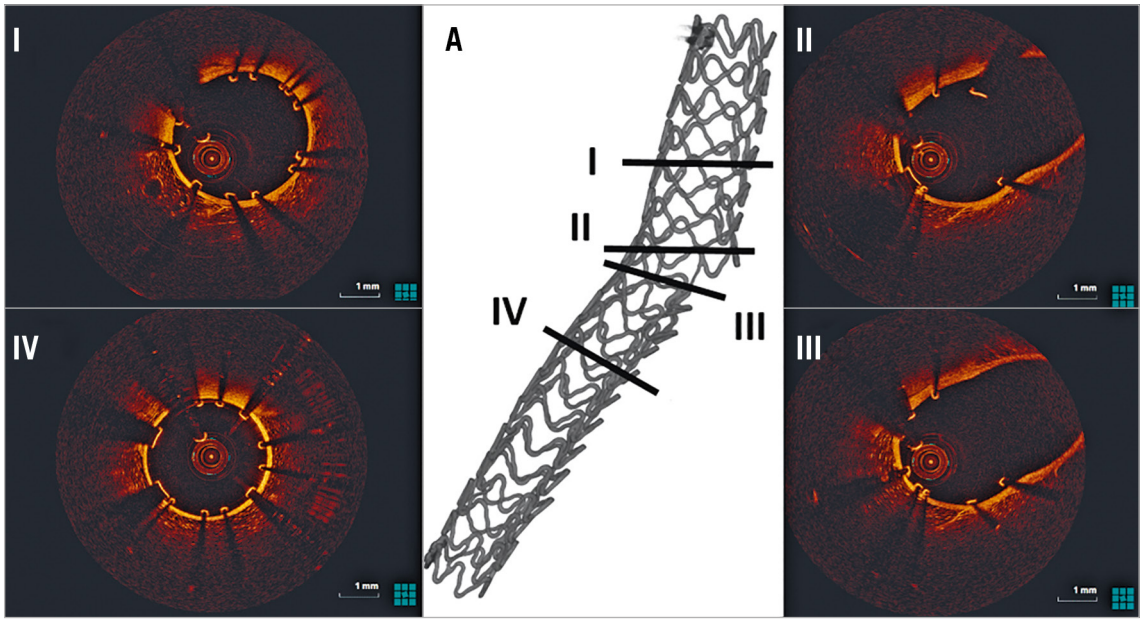

Figure 3. *OCT assessment following provisional stenting. A) 3D micro-CT reconstruction identifying the sites of OCT cross-sections. There is good strut apposition in the proximal (I) and distal (IV) MV. No inappropriately apposed MV struts opposite the SB ostium and good SB opening (II, III). MV: main vessel; SB: side branch*

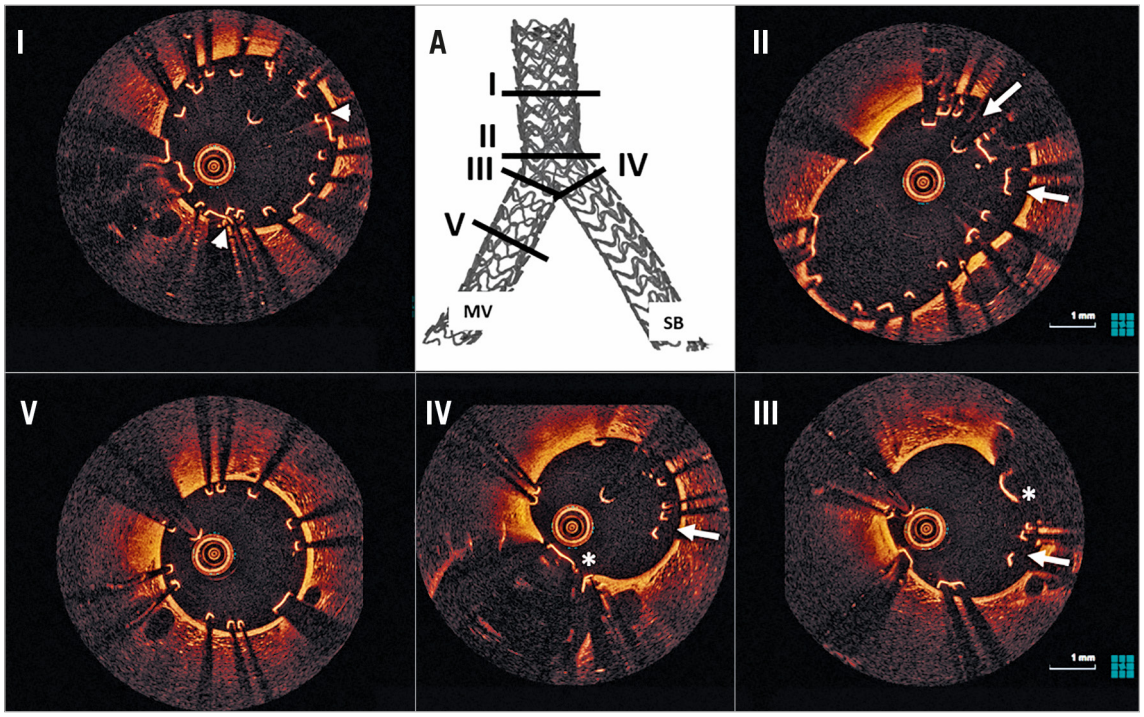

Figure 4. *OCT assessment following culotte stenting. A) 3D micro-CT reconstruction identifying the sites of OCT cross-sections. There is good scaffold expansion in all bifurcation segments (I-IV). In the proximal MV there is a double layer of struts (I, white arrowheads). At the level of the proximal bifurcation (II) there is a double layer of malapposed struts (white arrows). The neocarina (white *), composed of a double strut layer, is present at the MV (III) and SB side (IV), with several incompletely apposed struts present (III and IV, white arrows). There is good strut apposition in the distal MV (V). MV: main vessel; SB: side branch*

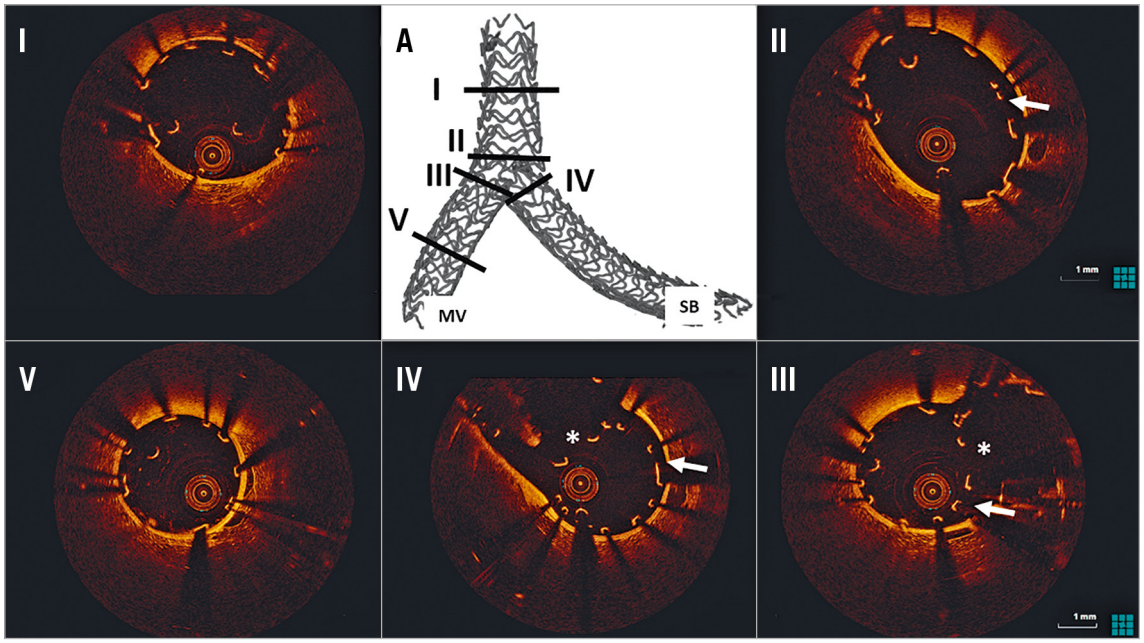

Figure 5. *OCT assessment following mod-T stenting. A) 3D micro-CT reconstruction identifying the sites of OCT cross-sections. There is good scaffold expansion in all bifurcation segments (I-IV). Several incomplete apposed struts are present in the proximal bifurcation segment (II, white arrow). The neocarina (white *), composed of a single strut layer, is present at the MV (III) and SB side (IV), with several inappropriately apposed struts (III and IV, white arrows). There is good strut apposition in the distal MV (V). MV: main vessel; SB: side branch*

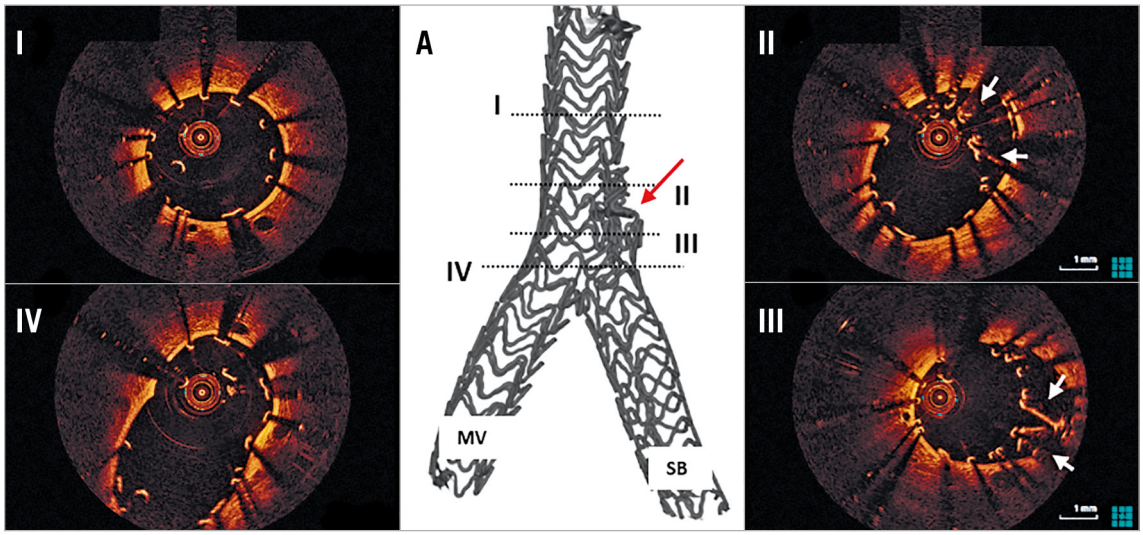

Figure 6. *OCT and micro-CT example of SB scaffold distortion following mod-T stenting. On micro-CT there is a bulky mesh of crushed SB scaffold just proximal to the origin of the SB (A, red arrow). On OCT, there is good scaffold expansion in the proximal main vessel (MV, I). A bundle of crushed, elongated and inappropriately apposed scaffold struts is evident (II, III, white arrows). In the proximal bifurcation segment (IV) there is complete bifurcation coverage. MV: main vessel; SB: side branch*

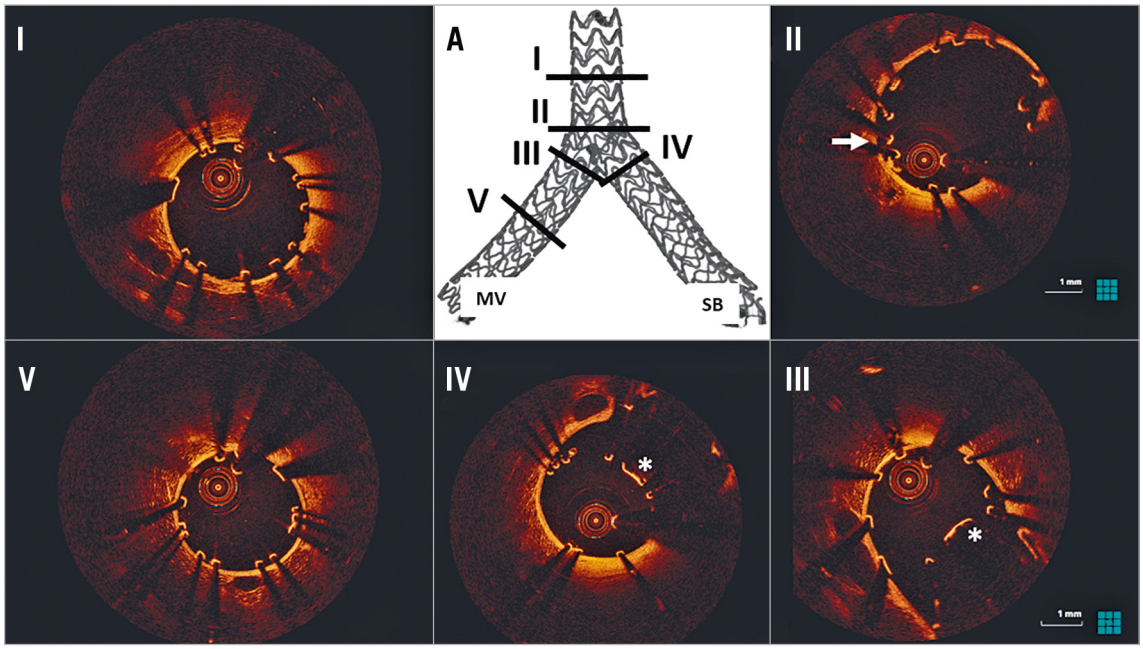

Figure 7. *OCT assessment following TAP stenting. A) 3D micro-CT reconstruction identifying the sites of OCT cross-sections. There is good scaffold expansion in all bifurcation segments (I-IV). There are several inappropriately apposed struts in the proximal bifurcation segment (II, white arrow). The neocarina (white *), composed of a single strut layer, is present at the MV (III) and SB side (IV), with no evidence of inappropriately apposed struts. There is good strut apposition in the distal MV (V). MV: main vessel; SB: side branch*

or both (n=1), with the connectors (n=4) and the rings (n=4) equally affected. There was no evidence of significant compromise to scaffold integrity following any procedure. Furthermore, there was only minimal luminal encroachment following two fractures.

PS WITH KBPD (N=5) (Moving image 1)

All PS procedures produced good results on 3D micro-CT assessment with scaffolding of all segments and good SB aperture. No strut fractures were identified.

Table 2. 3D micro-CT findings.

		Provisional		Culotte		mod-T		TAP	
		Trad (N=1)	Mini (N=4)	Trad (N=1)	Mini (N=5)	Trad (N=1)	Mini (N=5)	Trad (N=1)	Mini (N=7)
Proximal MV scaffold									
Strut fracture		0/1	0/4	0/1	0/5	0/1	1/5	1/1	0/7
No. of strut fractures/procedure							1/5	2	0
Ring							1/5	1	0
Connector								1	0
Distal MV scaffold									
Strut fracture		0/1	0/4	0/1	0/5	0/1	0/5	0/1	0/7
SB scaffold									
Strut fracture		0/1	0/4	0/1	0/5	0/1	0/5	0/1	0/7
Bifurcation segment									
Good aperture towards SB		1/1	4/4	1/1	5/5	1/1	4/5	1/1	7/7
Scaffold deformity		0/1	0/4	0/1	0/5	0/1	3/5	0/1	0/7
Multiple strut fractures		0/1	0/4	0/1	1/5	0/1	0/5	0/1	0/7
MV+SB scaffold affected					1/5				
MV scaffold	Ring						0/4		
	Connector					1/5			
SB scaffold	Ring								
	Connector					1/5			
Single strut fracture		0/1	0/4	1/1	2/5	0/1	1/5	0/1	2/7
MV scaffold affected				0/1			1/5		2/7
Ring									2/7
Connector							1/5		
SB scaffold affected				1/1	2/5				0/7
Ring					1/5				
Connector				1/1	1/5				
Luminal encroachment		0/1	0/4	0/1	0/5	0/1	2/5	0/1	0/7

MV: main vessel; SB: side branch; TAP: T and protrusion

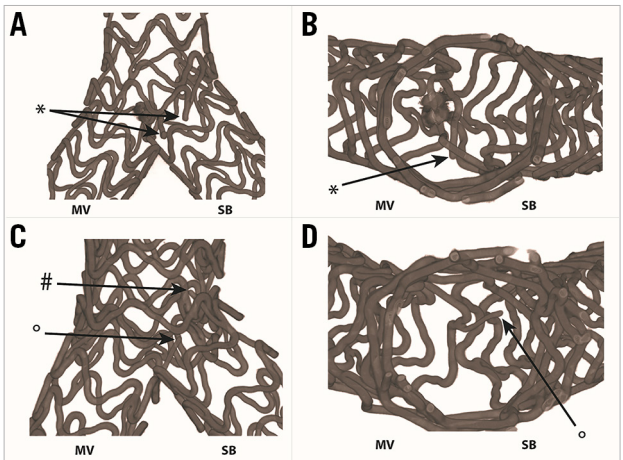

Figure 8. *3D micro-CT characteristics of strut fractures following TAP and culotte procedures. A single fracture is present following TAP stenting affecting an MV ring (A, black *) with no luminal compromise at the level of the carina (B, black *). Following culotte stenting, a fracture affecting an SB connector (C, black #), with no luminal compromise, whilst an additional fracture of an MV connector (C, black O) encroaches slightly on the lumen at the carina (D, black O). MV: main vessel; SB: side branch*

CULOTTE STENTING WITH KBPD (N=6) (Moving image 2)

On 3D micro-CT, all procedures produced good scaffolding and maintained good SB aperture. In the one culotte procedure with traditional KBPD, a single strut fracture was identified, whilst in the five culotte procedures with mini-KBPD two had single strut fractures and one had a double strut fracture. The single strut fractures affected only the SB. The double strut facture affected both an MV scaffold strut and an SB scaffold strut. Overall, the connectors (n=4) were more frequently affected than the rings (n=1). The fractures did not cause luminal compromise.

MODIFIED T-STENTING WITH KBPD (N=5) (Moving image 3)

All mod-T procedures produced good scaffolding and maintained good SB aperture. Strut fractures were identified following two of six mod-T stenting procedures, one at the level of the proximal MV and one at the bifurcation. The fracture at the bifurcation affected an MV connector with no luminal encroachment. Furthermore, in two cases there was scaffold deformity affecting the SB scaffold with a mesh of several layers of elongated and deformed struts located just proximal to the SB ostium **(Figure 4)**. This resulted in MV luminal encroachment in one case.

TAP STENTING WITH KBPD (N=8) (Moving image 4)

All TAP procedures produced good scaffolding and maintained good SB aperture. Multiple strut fractures were present in the proximal MV following one procedure, as described previously. Single strut fractures were present in two of eight procedures at the bifurcation level: these both occurred following the mini-KBPD strategy and in both instances affected the MV rings with evidence of minimal luminal encroachment in one case **(Figure 8D)**.

Discussion

The Magmaris is the first metal-based absorbable scaffold to be introduced into clinical practice. To date, it has been investigated in simple coronary artery lesions with encouraging 12-month clinical and angiographic results[7]. This is the first preclinical study to investigate the feasibility of performing more complex bifurcation procedures with the Magmaris by correlating findings on angiography, OCT and micro-CT.

The main observations are the following. 1) In a non-diseased bifurcation model, commonly used bifurcation techniques can be performed using the Magmaris with good angiographic results. 2) The SB can be easily wired with workhorse wires through single and double scaffold strut layers and the SB ostium can be crossed without difficulty with a balloon or second scaffold through an opened cell. 3) In all two-stent techniques, full bifurcation coverage and satisfactory scaffold expansion were achieved. 4) Angiography and 2D OCT are not able to detect the presence of strut fractures, unlike micro-CT (the gold standard). 5) POT of a 3.0 mm scaffold with a 3.5 mm NC balloon does not damage the scaffold integrity. 6) No strut fractures were identified following PS with KBPD, whilst in nine out of the 20 double-stent procedures single (n=7) or multiple (n=2) fractures were identified on 3D micro-CT. 7) Provisional and TAP stenting were the most promising techniques, with no scaffold distortion; single fractures were present following only two out of eight TAP procedures, with better SB ostium scaffold expansion on OCT after TAP compared to other two-stent techniques. 8) Modified T-stenting (technically mini mini-crush stenting) was more challenging, as delivering the MV scaffold past the crushed and minimally protruding SB scaffold was at times (two out of six procedures) difficult, creating a significant risk of important scaffold distortion of the proximal aspect of the SB scaffold. 9) Given the technical aspects of culotte stenting (extensive segment of double-layered struts proximally, double layer of thick struts at the bifurcation) and increased risk of strut fractures, this technique should probably be avoided with the current-generation Magmaris.

STRUT FRACTURES AND COMPROMISE OF SCAFFOLD INTEGRITY

In seven of the 25 stenting procedures, single strut fractures were identified, whilst in two procedures multiple strut fractures were identified. The majority of fractures were only discovered following very detailed analysis of the micro-CT images and 3D micro-CT reconstruction and were not identifiable on OCT as the affected struts presumably fell outward away from the lumen. The clinical importance of strut fractures is currently unknown. In two cases of mod-T stenting, there was important scaffold disruption affecting the proximal aspect of the SB scaffold, as a result of the MV scaffold getting entangled in struts protruding into the MV from the already deployed and crushed SB scaffold when attempting to deliver the MV scaffold. Although angiography did not reveal any obvious abnormality, OCT and micro-CT clearly identified a mesh of scaffold struts bundled together just proximal to the SB ostium **(Figure 6)**. In both instances, a soft resistance (see-sawing) was felt on delivering the MV scaffold past the "invisible" crushed SB scaffold, preventing the MV scaffold from passing. After further crushing of the SB scaffold with a larger balloon, the MV scaffolds passed without resistance. Nevertheless, SB scaffold disruption had already occurred in both cases, as noted on OCT imaging. In another case, a similar resistance was felt but slow rotational movement of the scaffold freed it from resistance and the scaffold was delivered with no ensuing scaffold distortion.

As fractured struts cannot be visualised by angiography, and in the majority of cases (unless there is significant distortion) also not by intravascular OCT, it is not possible to be sure of scaffold integrity following completion of two-stent bifurcation procedures using the Magmaris, as is the case with polymeric Absorb BVS[4].

Although no comparisons are made with metallic DES, strut fractures are not routinely observed following bifurcation stenting with current-generation metallic DES. Following two-stent procedures with the Magmaris, strut fractures were present at the bifurcation following seven out of 20 (35%) procedures. This compares favourably to the polymeric Absorb BVS where, following the same techniques in the same model, strut fractures at the level of the bifurcation were present in eight out of 15 (53%) procedures[4].

The presence of inappropriately apposed struts was observed. Every rabbit specimen is different, with variations in the size of arteries, whilst the scaffolds deployed were always the same size and post-dilatation strategies were predetermined. Therefore, in this study, adequate scaffold expansion is a more important observation. Underexpansion is known to trigger restenosis and thrombosis after metallic stent implantation[8], and after Absorb BVS implantation[9]. When performing bifurcation procedures, scaffold underexpansion must be avoided, as a double layer of 150 µm struts poorly expanded in the bifurcation would significantly increase the risk of early scaffold failure. The OCT observations in this acute non-calcified model would suggest that the Magmaris responds favourably to post-dilatation, with good expansion properties even when a double layer of struts is present.

WHICH BIFURCATION TECHNIQUE SHOULD BE AVOIDED/ RECOMMENDED?

As with metallic DES, PS is the default strategy in bifurcation lesions when using the Magmaris. POT, SB opening and KBPD generated good results on angiography, OCT and micro-CT in all PS procedures, with no strut fractures.

Although the angiographic results were good following culotte stenting, the OCT and micro-CT results were less satisfactory, with more frequent occurrence of single or double strut fractures. Moreover, a culotte strategy with the Magmaris leaves the patient with a double layer of thick scaffold struts in the proximal MV and bifurcation core, potentially impacting negatively on scaffold expansion in diseased calcific vessels. Therefore, culotte stenting with current-generation Magmaris should probably not be recommended for clinical practice.

In only one of six mod-T procedures was a single strut fracture present at the bifurcation. In this technique, the SB is stented before the MV, avoiding the need to pass one scaffold through another, thereby reducing potential damage to the integrity of the scaffolds. The downside of the technique is the difficulty in positioning the SB scaffold optimally, in order to minimise neocarina formation while avoiding suboptimal lesion coverage at the SB ostium. If the SB scaffold protrudes too much, the technique technically becomes a mini-crush/crush and increases the difficulty of delivering the MV scaffold. The use of multiple angiographic projections, as well as an optimal interpretation of the interplay of bifurcation angle and the radiopaque tantalum markers, may improve implantation success. Nevertheless, given the occurrence of important SB scaffold distortion following two cases, this technique should probably be avoided in clinical practice.

In our analysis, TAP stenting appeared the most promising and the safest option when using two Magmaris. At the bifurcation, only single strut fractures were identified on micro-CT, with no significant luminal compromise. Furthermore, there was good scaffold expansion, especially at the SB ostium, and long segments of double struts were avoided. In terms of fluoroscopy time, TAP stenting was slightly longer than PS but significantly shorter than culotte or mod-T stenting. These findings need to be confirmed in clinical studies.

Limitations

Although *in vivo* preclinical testing provides valuable insights, the non-diseased model used may not accurately predict scaffold behaviour in humans. Furthermore, the long-term outcomes need to be assessed, especially as the clinical implications of one or two strut fractures are unknown. Unfortunately, this model only allows a single micro-CT scaffold assessment post dissection of the aorto-iliac bifurcation, thus not allowing serial assessments over a longer time frame which may provide interesting data on sequelae of strut fractures. The rabbit aorto-iliac bifurcation model has a relatively high-angle bifurcation and therefore does not allow assessment at differing angles, meaning that results cannot be translated to all bifurcations. This model does not allow comprehensive assessment of strut apposition on OCT as there is inter-animal variation in anatomy. The current study included relatively small numbers of animals that may not reveal significant differences between treatment groups.

Conclusions

BRS technology represents an important new development in the management of simple and, hopefully, complex coronary artery disease. This preclinical acute *in vivo* study provides valuable insights into the opportunities and limitations of the magnesium alloy Magmaris in coronary bifurcations. In a non-diseased rabbit bifurcation model, it was feasible to perform complex bifurcation stenting using the Magmaris with good angiographic results. PS of the MV, with additional TAP stenting whenever needed, seems a reasonable approach for bifurcation lesions. Whenever a two-stent technique is required, again the TAP technique would appear to be the most favourable technique. Furthermore, based on scaffold behaviour in our analysis, mod-T and culotte stenting strategies employing current-generation Magmaris should rather be discouraged.

Impact on daily practice

Complex bifurcation stenting using the Magmaris is feasible in a non-diseased animal model; however, this study highlights concerns that scaffold integrity may be compromised during complex bifurcation procedures. Clinical studies are needed to assess whether the results obtained in this non-diseased model translate to human diseased coronary arteries and, more importantly, to assess the acute and long-term clinical outcomes of this new technology.

Funding

This study was an independent, investigator-initiated study. A research grant was awarded by Biotronik AG (Bülach, Switzerland) to cover the study costs.

Conflict of interest statement

J. Bennett and C. Dubois are holders of research grants from Biotronik AG. The other authors have no conflicts of interest to declare.

References

1. Collins N, Seidelin P, Daly P, Ivanov J, Barolet A, Mackie K, Bui S, Schwartz L, Dzavík V. Long-term outcomes after percutaneous coronary intervention of bifurcation narrowings. *Am J Cardiol.* 2008;102:404-10.

2. Iakovou I, Schmidt T, Bonizzoni E, Ge L, Sangiorgi GM, Stankovic G, Airoldi F, Chieffo A, Montorfano M, Carlino M, Michev I, Corvaja N, Briguori C, Gerckens U, Grube E, Colombo A. Incidence, predictors, and outcome of thrombosis after successful implantation of drug-eluting stents. *JAMA.* 2005; 293:2126-30.

3. Ormiston JA, Webber B, Ubod B, Webster MW, White J. Absorb everolimus-eluting bioresorbable scaffolds in coronary bifurcations: a bench study of deployment, side branch dilatation and post-dilatation strategies. *EuroIntervention.* 2015;10:1169-77.

4. Bennett J, Vanhaverbeke M, Vanden Driessche N, Adriaenssens T, Hiltrop N, Desmet W, Sinnaeve P, Dubois C. Absorb Bioresorbable Vascular Scaffold in Complex Coronary Bifurcation Interventions: Insights From an In Vivo Multimodality Imaging Study. *Circ Cardiovasc Interv.* 2016 Aug;9(8).

5. Schmidt W, Behrens P, Brandt-Wunderlich C, Siewert S, Grabow N, Schmitz KP. In vivo performance investigation of bioresorbable scaffolds – Standard tests for vascular stents and beyond. *Cardiovasc Revasc Med.* 2016;17:375-83.

6. Campos CM, Muramatsu T, Iqbal J, Zhang YJ, Onuma Y, Garcia-Garcia HM, Haude M, Lemos PA, Warnack B, Serruys PW. Bioresorbable drug-eluting magnesium alloy scaffold for treatment of coronary artery disease. *Int J Mol Sci.* 2013;14:24492-500.

7. Haude M, Ince H, Abizaid A, Toelg R, Lemos PA, von Birgelen C, Christiansen EH, Wijns W, Neumann FJ, Kaiser C, Eeckhout E, Lim ST, Escaned J, Onuma Y, Garcia-Garcia HM, Waksman R. Sustained safety and performance of the second-generation drug-eluting absorbable metal scaffold in patients with de novo coronary lesions: 12-month clinical results and angiographic findings of the BIOSOLVE-II first-in-man trial. *Eur Heart J.* 2016; 37:2701-9.

8. Fujii K, Mintz GS, Kobayashi Y, Carlier SG, Takebayashi H, Yasuda T, Moussa I, Dangas G, Mehran R, Lansky AJ, Reyes A, Kreps E, Collins M, Colombo A, Stone GW, Teirstein PS, Leon MB, Moses JW. Contribution of stent underexpansion to recurrence after sirolimus-eluting stent implantation for in-stent restenosis. *Circulation.* 2004;109:1085-8.

9. Longo G, Granata F, Capodanno D, Ohno Y, Tamburino CI, Capranzano P, La Manna A, Francaviglia B, Gargiulo G, Tamburino C. Anatomical features and management of bioresorbable vascular scaffolds failure: A case series from the GHOST registry. *Catheter Cardiovasc Interv.* 2015;85:1150-61.

Supplementary data

Moving image 1. 3D micro-CT reconstruction following provisional stenting.

Moving image 2. 3D micro-CT reconstruction following culotte stenting.

Moving image 3. 3D micro-CT reconstruction following mod-T stenting.

Moving image 4. 3D micro-CT reconstruction following TAP stenting.

The supplementary data are published online at: http://www.pcronline.com/eurointervention/132nd_issue/333